Advances in Analysis and Applied Mathematics, **2**(2) (2025), 119–131.

https://doi.org/10.62298/advmath.36

ISSN Online: 3062-0686 / Open Access

ADVANCES IN ANALYSIS AND APPLIED MATHEMATICS

Check for updates

Research Paper

High-Accuracy Finite Element Modeling of the Rosenau–Hyman Equation

Derya Yıldırım Sucu[1,*]

[1]Department of Mathematics, Nevşehir Hacı Bektaş Veli University, 50300, Nevşehir, Türkiye,

*To whom correspondence should be addressed: deryasucu@aksaray.edu.tr

Received 7 October 2025; Revised 23 November 2025; Accepted 28 December 2025; Published 31 December 2025

Abstract

The present study focuses on the numerical solution of the Rosenau–Hyman (R–H) equation, also known as the generalized Korteweg–de Vries equation, which describes the dynamics of shallow water waves and pattern formation in liquid drops. To this end, a collocation finite element method based on septic B-spline approximation is proposed and applied to the R–H equation for different parameter values of the test problem. In addition, a von Neumann stability analysis is performed, demonstrating that the proposed scheme is unconditionally stable. The efficiency and reliability of the method are illustrated by solving a test problem and computing the L_2 and L_∞ error norms. The numerical results are found to be in very good agreement with the corresponding analytical solutions, indicating that the proposed B-spline collocation algorithm is both accurate and robust. To further demonstrate the effectiveness of the method in solving nonlinear equations, the results are presented graphically as well as in tabular form. The close consistency between analytical and numerical results suggests that the proposed approach is a powerful and attractive tool for investigating characteristic features of nonlinear phenomena in various fields of science.

Key Words: Rosenau–Hymann equation; Collocation; Septic B-spline; Finite element method

AMS 2020 Classification: 65N30; 65D07; 74S05; 74J35; 76B25

1. Introduction

The theory of nonlinear phenomena is known as one of the most critical fields of scientific research. In recent years, researchers have extensively discussed various mathematical models such as the KdV equation

$$U_t + aUU_x + bU_{xxx} = 0, \tag{1}$$

which has been used as a model for unidirectional, long, dispersive waves [1, 2], the RLW (Regularized Long Wave) equation

$$U_t + U_x + aUU_x - bU_{xxt} = 0, \tag{2}$$

that has been analyzed widely by Benjamin et al. [3] and others [4]-[16], and the Rosenau equation

$$U_t + U_x + U_{xxxxt} + UU_x = 0, \tag{3}$$

which was introduced to describe the dynamics of dense discrete systems [17]. Although Eq. (1) has a wide range of application areas, it also has several shortcomings [18, 19]. To overcome these shortcomings of Eq. (1), Eq. (3) was proposed by Philip Rosenau in 1988 [20]. The existence and uniqueness of Eq. (3) were demonstrated by Park [21, 22] and Barreto et al. [23]. Besides theoretical investigations, numerical analyses of Eq. (3) also exist in the literature; see [24]-[28] and the references therein.

As is well known, Eq. (1), which was discovered to identify water wave motion in channels, is a significant nonlinear partial differential equation (NLPDE) possessing soliton solutions. Similarly, other PDEs related to fluid mechanics and plasma physics phenomena also admit soliton solutions [29]. Compactons are traveling wave solutions with compact support, resulting from a balance between nonlinearity and nonlinear dispersion. These solutions were first observed in a generalized KdV equation with nonlinear dispersion, known as the $K(p,p)$ compacton equation of Rosenau and Hyman [30], given by

$$U_t - c_0 U_x + \sigma(U^p)_x + \mu(U^p)_{xxx} = 0, \tag{4}$$

where c_0 is a constant velocity introduced to stop the compacton when necessary. Compactons also preserve their shape after collisions [31]. Equation (4) has been explored as a simplified model for studying the role of nonlinear dispersion in pattern formation in liquid drops [32], and compactons have various applications in physics and science [33]-[36].

Numerical approaches indicate that an initial pulse wider than a compacton separates into a set of compactons accompanied by a small amount of radiation. Moreover, compactons collide elastically, suffering only a phase shift after the collision and producing zero-mass, small-amplitude compact ripples [37, 38, 39, 40, 41]. Numerical solutions of Eq. (4) are relatively limited in the literature. The most widely used numerical techniques are pseudospectral methods in space [30, 42]. Finite element methods based on cubic B-splines [37], methods based on piecewise polynomials discontinuous at the element interfaces [43], high-order Padé methods [38], second-order finite difference methods [44], and the method of lines with adaptive mesh refinement [45] have also been applied successfully. These studies motivate us to analyze the R–H equation and further investigate its numerical properties. Several other numerical methods [46]-[55] have been implemented to solve fractional models of this type of equation.

In order to obtain numerical solutions for real-life problems arising in different fields of science, it is crucial to choose an efficient and reliable numerical approach. The Finite Element Method (FEM), which is one of the most effective techniques for solving boundary-value problems in approximation theory, is particularly noteworthy. In this study, a B-spline-based collocation method has been chosen as the interpolation framework due to its computational efficiency and ease of implementation. Motivated by these advantages, a reliable and efficient numerical scheme is implemented to obtain new numerical solutions of the equation.

The remainder of the paper is organized as follows. In Section 2, the B-spline basis functions are introduced, and the proposed numerical scheme is formulated and applied to the governing equation. The stability analysis of the numerical method is presented in Section 3. In Section 4, a fully discrete algorithm is constructed and its convergence properties are briefly discussed. In Section 5, a test problem taken from the literature is solved, and the corresponding numerical results are presented in both tabular and graphical forms. Finally, concluding remarks are given in the last section.

2. Numerical Calculations

In this section, Eq. (4) is solved using the septic B-spline collocation method. The septic B-spline functions $\phi_m(x)$, $m = -3(3)N$, defined at the nodes x_m over the solution interval $[a, b]$, are constructed following the approach presented in [57]. Among various numerical techniques, the collocation method is well known for improving numerical accuracy due to its advantageous properties.

In the collocation method, the numerical approximation $U_{numeric}(x,t)$ corresponding to the exact solution $U_{exact}(x,t)$ is expressed as a linear combination of septic B-spline interpolation functions as

$$U_{numeric}(x,t) = \sum_{m=-3}^{N+3} \phi_m(x)\rho_m(t). \tag{5}$$

When the transformation $h\rho = x - x_m$, $(0 \leq \rho \leq 1)$ is applied over the finite region $[x_m, x_{m+1}]$, this region is mapped onto the interval $[0, 1]$. Consequently, the septic B-spline functions defined on the new region $[0, 1]$ are obtained as follows:

$$
\begin{aligned}
\phi_{m-3} &= 1 - 7\rho + 21\rho^2 - 35\rho^3 + 35\rho^4 - 21\rho^5 + 7\rho^6 - \rho^7, \\
\phi_{m-2} &= 120 - 392\rho + 504\rho^2 - 280\rho^3 + 84\rho^5 - 42\rho^6 + 7\rho^7, \\
\phi_{m-1} &= 1191 - 1715\rho + 315\rho^2 + 665\rho^3 - 315\rho^4 - 105\rho^5 + 105\rho^6 - 21\rho^7, \\
\phi_{m} &= 2416 - 1680\rho + 560\rho^4 - 140\rho^6 + 35\rho^7, \\
\phi_{m+1} &= 1191 + 1715\rho + 315\rho^2 - 665\rho^3 - 315\rho^4 + 105\rho^5 + 105\rho^6 - 35\rho^7, \\
\phi_{m+2} &= 120 + 392\rho + 504\rho^2 + 280\rho^3 - 84\rho^5 - 42\rho^6 + 21\rho^7, \\
\phi_{m+3} &= 1 + 7\rho + 21\rho^2 + 35\rho^3 + 35\rho^4 + 21\rho^5 + 7\rho^6 - \rho^7, \\
\phi_{m+4} &= \rho^7.
\end{aligned} \tag{6}
$$

Using the equalities given by (5) and (7), following expressions are obtained:

$$
\begin{aligned}
U_N(x_m, t) = U_m &= \rho_{m-3} + 120\rho_{m-2} + 1191\rho_{m-1} + 2416\rho_m + 1191\rho_{m+1} + 120\rho_{m+2} + \rho_{m+3}, \\
U'_m &= \frac{7}{h}\left(-\rho_{m-3} - 56\rho_{m-2} - 245\rho_{m-1} + 245\rho_{m+1} + 56\rho_{m+2} + \rho_{m+3}\right), \\
U''_m &= \frac{42}{h^2}\left(\rho_{m-3} + 24\rho_{m-2} + 15\rho_{m-1} - 80\rho_m + 15\rho_{m+1} + 24\rho_{m+2} + \rho_{m+3}\right), \\
U'''_m &= \frac{210}{h^3}\left(-\rho_{m-3} - 8\rho_{m-2} + 19\rho_{m-1} - 19\rho_{m+1} + 8\rho_{m+2} + \rho_{m+3}\right), \\
U^{iv}_m &= \frac{840}{h^4}\left(\rho_{m-3} - 9\rho_{m-1} + 16\rho_m - 9\rho_{m+1} + \rho_{m+3}\right).
\end{aligned} \tag{7}
$$

Now, putting (5) and (8) in Eq.(4) and simplifying, following system of ODEs are reached:

$$
\begin{aligned}
& \dot{\rho}_{m-3} + 120\dot{\rho}_{m-2} + 1191\dot{\rho}_{m-1} + 2416\dot{\rho}_m + 1191\dot{\rho}_{m+1} + 120\dot{\rho}_{m+2} + \dot{\rho}_{m+3} \\
- & \frac{210}{h^3} Z_1 \left(-\rho_{m-3} - 8\rho_{m-2} + 19\rho_{m-1} + 19\rho_{m+1} + 8\rho_{m+2} + \rho_{m+3}\right) \\
- & \frac{7}{h} Z_1 \left(-\rho_{m-3} - 56\rho_{m-2} - 245\rho_{m-1} + 245\rho_{m+1} + 56\rho_{m+2} + \rho_{m+3}\right) \\
- & \frac{126}{h^2} Z_2 \left(\rho_{m-3} + 24\rho_{m-2} + 15\rho_{m-1} - 80\rho_m + 15\rho_{m+1} + 24\rho_{m+2} + \rho_{m+3}\right) = 0.
\end{aligned} \tag{8}
$$

where

$$
\begin{aligned}
Z_1 &= U_m = \rho_{m-3} + 120\rho_{m-2} + 1191\rho_{m-1} + 2416\rho_m + 1191\rho_{m+1} + 120\rho_{m+2} + \rho_{m+3}, \\
Z_2 &= U'_m = \frac{7}{h}\left(-\rho_{m-3} - 56\rho_{m-2} - 245\rho_{m-1} + 245\rho_{m+1} + 56\rho_{m+2} + \rho_{m+3}\right).
\end{aligned}
$$

If Crank-Nicolson scheme and forward difference approximation which are defined below is used respectively in Eq.(9)

$$
\rho_i = \frac{\rho_i^{n+1} + \rho_i^n}{2}, \; \dot{\rho}_i = \frac{\rho_i^{n+1} - \rho_i^n}{\Delta t} \tag{9}
$$

the following iteration equation is obtained

$$
\gamma_1\rho_{m-3}^{n+1} + \gamma_2\rho_{m-2}^{n+1} + \gamma_3\rho_{m-1}^{n+1} + \gamma_4\rho_{m}^{n+1} + \gamma_5\rho_{m+1}^{n+1} + \gamma_6\rho_{m+2}^{n+1} + \gamma_7\rho_{m+3}^{n+1} \tag{10}
$$

$$= \gamma_7\rho^n_{m-3} + \gamma_6\rho^n_{m-2} + \gamma_5\rho^n_{m-1} + \gamma_4\rho^n_m + \gamma_3\rho^n_{m+1} + \gamma_2\rho^n_{m+2} + \gamma_1\rho^n_{m+3}.$$

where

$$\begin{aligned}
\gamma_1 &= [1 + A + B - C], \\
\gamma_2 &= [120 + 8A + 56B - 24C], \\
\gamma_3 &= [1191 - 19A + 245B - 15C], \\
\gamma_4 &= [2416 + 80C], \\
\gamma_5 &= [1191 + 19A - 245B - 15C], \\
\gamma_6 &= [120 - 8A - 56B - 24C], \\
\gamma_7 &= [1 - A - B - C], \\
m &= 0, 1, \ldots, N, \\
A &= \frac{105\Delta t}{h^3}Z_1, \quad B = \frac{7\Delta t}{2h}Z_1, \quad C = \frac{63\Delta t}{h^2}Z_2.
\end{aligned} \tag{11}$$

To assure a unique solution, it is necessary to eliminate unknown parameters $(\rho_{-3}, \rho_{-2}, \rho_{-1}, \rho_{N+1}, \rho_{N+2}, \rho_{N+3})^T$ from the resulting system (11). This procedure can be easily done using the values of u and boundary conditions, and then following system

$$R\mathbf{d^{n+1}} = S\mathbf{d^n} \tag{12}$$

is obtained where $d^n = (\rho_0, \rho_1, ..., \rho_N)^T$.

3. Stability Analysis

For the stability analysis, Von Neumann technique has been used. In a typical amplitude mode, we can define the magnification factor ξ of the error as follows

$$\rho^n_m = \xi^n e^{ikmh}. \tag{13}$$

Using (13) into the (11),

$$\xi = \frac{\omega_1 + i\omega_2}{\omega_1 - i\omega_2},$$

is procured where

$$\begin{aligned}
\omega_1 &= (2382 - 30C)\cos(kh) + (240 - 48C)\cos(2kh) + (2 - 2C)\cos(3kh) + (2416 + 80C) \\
\omega_2 &= (-38A + 490B)\sin(kh) + (16A + 112B)\sin(2kh) + (2A + 2B)\sin(3kh)
\end{aligned}$$

so that $|\xi| = 1$, which shows unconditional stability of the linearized numerical scheme for the Rosenau-Hymann equation.

4. Convergence: A Fully Discrete Algorithm

A higher-order B-spline collocation technique is employed in space, together with an appropriate time discretization scheme, to approximate the nonlinear partial differential equation (4). The efficiency of a computational algorithm is commonly evaluated in terms of accuracy, numerical flexibility, and ease of implementation. Accordingly, this section outlines the fundamental ideas underlying the proposed approach and summarizes the main results, while omitting detailed proofs. For a more comprehensive theoretical treatment, the reader is referred to the existing literature.

More specifically, a brief discussion on the validity of the space–time scheme introduced above is provided without presenting a formal proof. A rigorous and well-established theoretical background can be found in [58, 59] and the references therein. It should be emphasized that the constants $C_i \geq 0$ appearing in the analysis are generic and may differ from one estimate to another.

Global polynomial interpolation methods are well suited for problems in which the underlying solutions are sufficiently smooth and the computational domain is simple. However, many physical and engineering problems are defined on complex domains, where finite element approximations offer a more robust and accurate representation of the solution behavior.

A key property of piecewise polynomial basis functions in approximation theory is their smoothness over all user-defined subintervals, which makes them particularly advantageous for the analysis of approximate solutions. On each spatial subinterval, $p+1$ data values are available; consequently, there exists a polynomial of degree at most p that interpolates these data points. The approximation error associated with such polynomial representations depends on the spacing between the data points, commonly denoted by h. As a consequence, the proposed technique exhibits superconvergence at the collocation points [60]. Here, $H^r(\Omega)$ denotes the space of r-times differentiable functions, $\|\cdot\|_r$ represents the standard $H^r(\Omega)$ norm, and $\|\cdot\|_0$ denotes the $L_2(\Omega)$ norm.

Let v_h be an approximation to a function $v(x) \in H^k(\Omega)$ in Ω. Also h is distance between the grids and $\Omega = \cup_i \Omega_i$, where $\Omega_i = [x_i,\ x_{i+1}]$, $x_{i+1} = x_i + h$. It is clear to notice [61, 62] that

$$\|v(x) - v_h(x)\| \leq Ch^{p+1}\|v\|_{p+1} \text{ where } 1 \leq p < k.$$

It follows that

$$\|w(x) - w_h(x)\| \leq Ch^{m+1}\|w\|_{m+1} \text{ where } 1 \leq m < p,$$

is well established. For each $w \in H_p(\Omega)$, if w_h is an appropriate $B-$spline identified by a polynomial of degree less or equal k. In this current spatial approximation, septic B-splines are utilized.

It follows that, in $L_2(\Omega)$ [63], a theoretical $\mathcal{O}(h^8)$ accuracy is obtained from such a spatial approximation. Here, for some $T > 0$, a forward difference scheme of $\mathcal{O}(h^8)$ in $L_2([0,T])$ norm is accurate. The accuracy for the entire discrete scheme can therefore be expressed as follows:

$$|u(x,t) - u_h(x,tl)| \leq C_1 h^8 + C_2,$$

with an appropriate $C_1 \geq 0$ and $C_2 \geq 0$.

5. Numerical Applications and Discussions

In this section, the proposed numerical scheme is implemented to obtain solutions of the Rosenau–Hyman equation for various choices of spatial and temporal discretization parameters. The approximate solutions are computed using the formulation developed in the previous sections. To assess the accuracy and reliability of the proposed method, standard error measures widely adopted in the literature are employed, namely the L_2 and L_∞ error norms. These norms provide a quantitative evaluation of the global and maximum pointwise errors, respectively, and thus offer a clear indication of the performance and convergence behavior of the numerical scheme.

$$L_2 = \|U_{exact} - U_{numeric}\|_2 \simeq \sqrt{h\sum_{j=1}^{N}\left|U_j^{exact} - (U_{numeric})_j\right|^2}, \tag{14}$$

$$L_\infty = \|U_{exact} - U_{numeric}\|_\infty \simeq \max_j \left|U_j^{exact} - (U_{numeric})_j\right|, \quad j = 1, 2, ..., N. \tag{15}$$

Rosenau-Hymann equation is considered for the parameters $p = 2$, $\sigma, \mu = -\frac{1}{2}$. In this case, Eq. 4 is written as:

$$U_t - UU_x - UU_{xxx} - 3U_xU_{xx} = 0 \tag{16}$$

Analytical form of the Eq. (4) is

$$U(x,t) = -\frac{8c}{3}\cos^2(\frac{x-ct}{4}), \tag{17}$$

and the initial condition is

$$U(x,0) = -\frac{8c}{3}\cos^2(\frac{x}{4}).$$

To demonstrate the accuracy of the proposed numerical algorithm, the computational domain is chosen as $[x_L = -10, x_R = 10]$ in Eq. (16). The final simulation time is taken as $t = 10$, in accordance with similar studies reported in the literature.

In the numerical simulations, commonly adopted discretization parameters in the literature, namely $\Delta t = 0.01$, 0.001 and $h = 1$, 0.1, are selected to ensure a consistent and meaningful comparison with existing studies. The numerical solutions obtained by the proposed scheme are presented alongside the corresponding exact solutions in order to assess the accuracy of the method.

		$\Delta t = 0.01, h = 0.1$	
t	x	$U_{exact}(x,t)$	$U_{numeric}(x,t)$
[64] $t = 0.3$	0.3	-.265169	-.265168
[65] $t = 0.3$	0.3	-.265453	-.265453
0.3	0.3	-.265452	-.265168
0.3	1.0	-.251285	-.250340
0.3	1.6	-.227645	-.226221
1.0	0.3	-.265999	-.265168
1.0	1.0	-.253389	-.250340
1.0	1.6	-.230885	-.226221
1.6	0.3	-.266339	-.265168
1.6	1.0	-.255074	-.250340
1.6	1.6	-.233568	-.226221
2.0	0.3	-.266499	-.265168
2.0	1.0	-.256138	-.250340
2.0	1.6	-.235306	-.226221

Table 1. Numerical results at the collocation points of example 1 for $h = 0.1$ and $\Delta t = 0.01$.

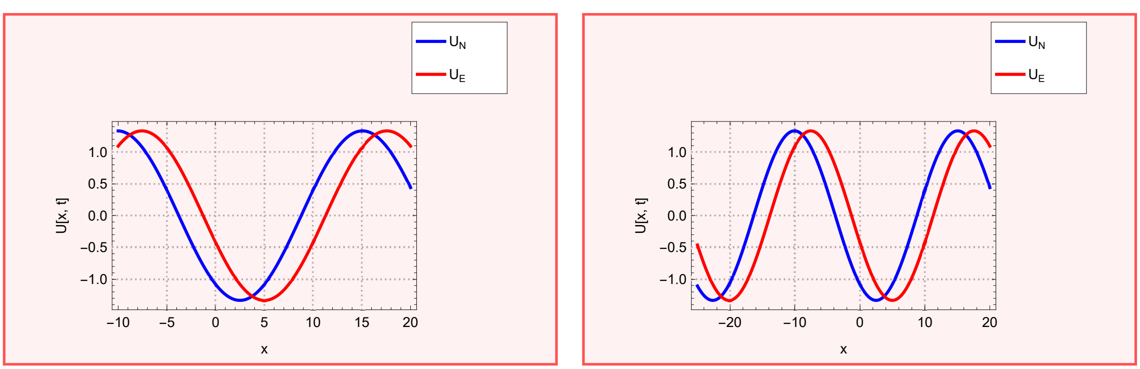

Fig. 1. Comparison of numerical solution for $\Delta t = 0.01$ and $h = 0.1$ with the exact solution.

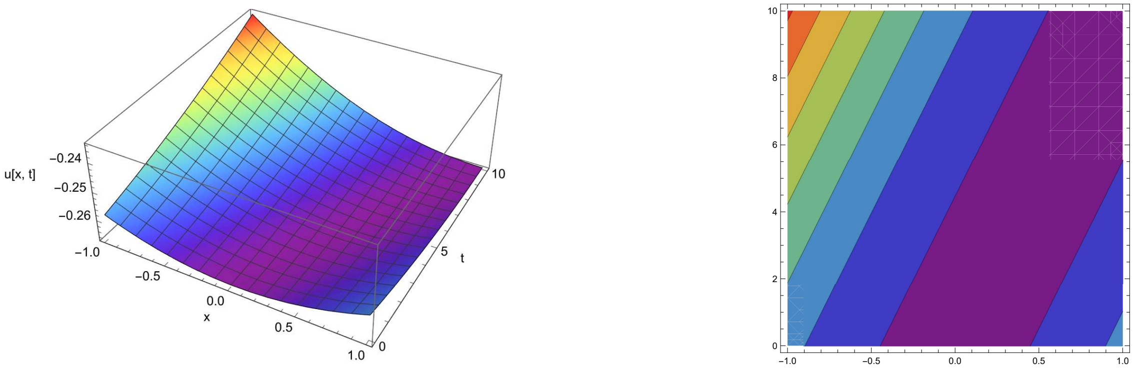

Fig. 2. The surface plots of numerical solutions of the problem and Contour plot for $\Delta t = 0.01$ and $h = 0.1$ at $x \in [-1, 1]$.

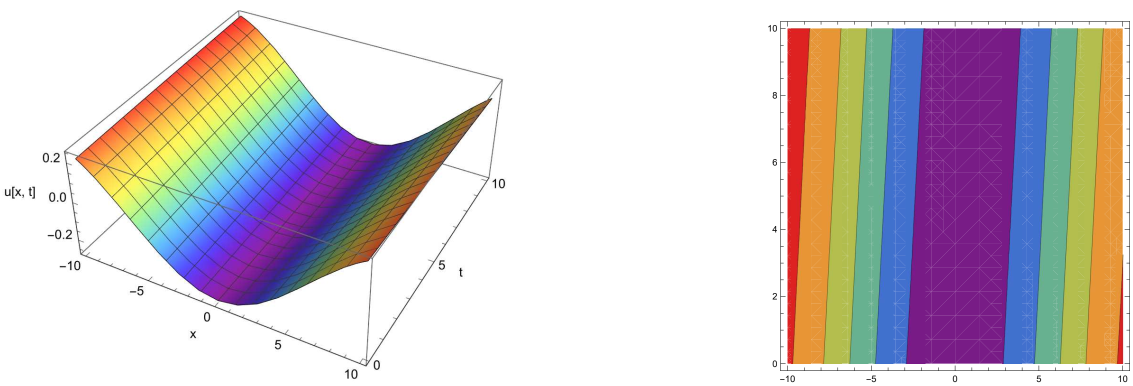

Fig. 3. The surface plots of numerical solutions of the problem and Contour plot for $\Delta t = 0.01$ and $h = 1$ at $x \in [-10, 10]$.

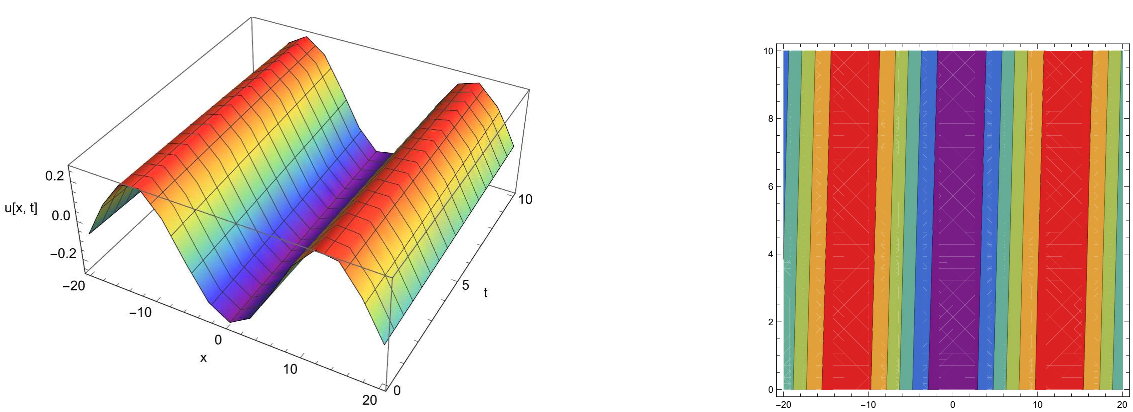

Fig. 4. The surface plots of numerical solutions of the problem and Contour plot for $\Delta t = 0.001$ and $h = 1$ at $x \in [-20, 20]$.

		$\Delta t = 0.01, h = 0.1$		$\Delta t = 0.01, h = 1$	
t	c	$L_2 - Error$	$L_\infty - Error$	$L_2 - Error$	$L_\infty - Error$
[64]	0.5	1.81E-02	2.68E-02	1.81E-02	2.68E-02
0.1	0.5	2.165E-04	6.666E-05	2.252E-06	6.650E-07
0.3	0.5	6.497E-04	1.999E-04	6.757E-06	1.995E-06
0.5	0.5	1.082E-03	3.332E-04	1.126E-05	3.325E-06
1.0	0.5	2.165E-03	6.665E-04	2.252E-05	6.651E-06
1.5	0.01	3.247E-03	9.997E-04	3.378E-05	9.977E-06
3.0	0.01	6.497E-05	1.999E-05	6.757E-05	1.995E-05
5.0	0.01	1.082E-04	3.332E-04	1.126E-04	3.327E-05
7.0	0.01	1.515E-04	4.667E-05	1.576E-04	4.659E-05
10.0	0.01	2.165E-04	6.665E-05	2.252E-04	6.658E-05
50.0	0.01	1.083E-03	3.324E-04	6.720E-04	2.094E-04
100.0	0.01	2.144E-03	6.596E-04	6.778E-04	2.115E-04

Table 2. The Absolute Error Norms at the collocation points of test problem for different values of h and $\Delta t = 0.01$.

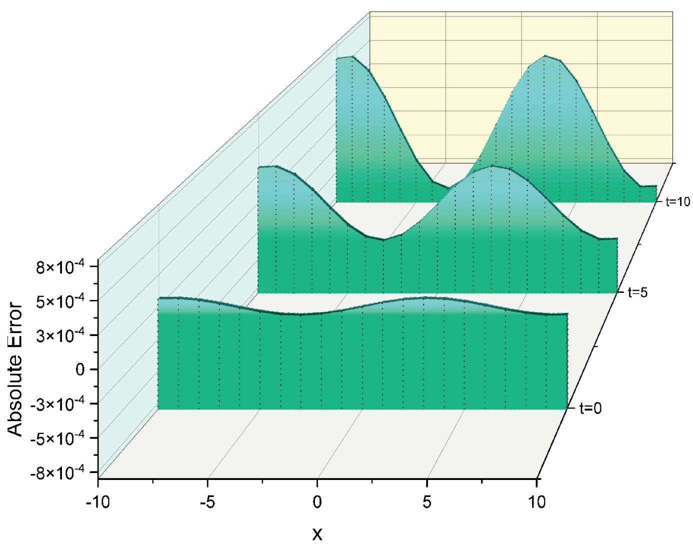

Fig. 5. Absolute error norms of the problem for $\Delta t = 0.01$ and $h = 1$.

Furthermore, the numerical values reported in Table 1 are directly compared with those available in [64] and [65] for the case $h = 0.1$. The comparison reveals an excellent agreement between the present results and the referenced solutions, thereby confirming the reliability of the proposed approach. In several instances, the computed errors are observed to be smaller, indicating an improvement in accuracy.

Figure 1 depicts a two-dimensional graphical comparison between the numerical and exact solutions over the time interval $0 \leq t \leq 10$, demonstrating that the proposed method accurately captures the solution behavior throughout the evolution process. In addition, Figures 2, 3 and 4 display three-dimensional surface plots of the numerical solutions for different choices of h and Δt, together with their corresponding contour plots, which further illustrate the stability and convergence characteristics of the method.

Overall, the numerical results presented in both tabular and graphical forms clearly indicate that the proposed technique provides more accurate and reliable approximations than several existing methods reported in the literature.

Table 2 reports the values of the L_2 and L_∞ error norms computed for different time levels and step sizes. These results clearly illustrate the influence of the discretization parameters on the behavior and accuracy of the numerical scheme. A careful examination of the table shows that both error norms remain consistently small, indicating the stability and high accuracy of the proposed method. Moreover, a noticeable reduction in the error values is observed as the number of temporal subdivisions increases, demonstrating the favorable impact of time refinement on the numerical performance.

To facilitate a direct comparison with previously published studies, the computations are extended up to $t = 100$. Table 2 provides a detailed comparison between the results obtained by the present method and those reported in Ref. [64]. It is evident from this comparison that the proposed collocation-based approach, combined with the adopted discretization strategy, yields more accurate and reliable results than the existing methods.

In addition, the absolute errors corresponding to $\Delta t = 0.01$ and $h = 1$ at selected time levels are depicted in Figure 5. This figure clearly demonstrates that the numerical accuracy improves as the spatial step size h decreases, confirming the convergence behavior of the proposed scheme.

6. Conclusion

In this paper, a collocation finite element method based on septic B-spline basis functions has been presented for the numerical solution of the nonlinear Rosenau–Hyman equation. The stability of the proposed scheme has been rigorously investigated via the von Neumann stability analysis, establishing its unconditional stability. The accuracy and effectiveness of the method have been verified through several numerical experiments, where absolute error norms were computed and the results were compared with those reported in the existing literature. The obtained numerical results demonstrate that the proposed approach yields highly accurate approximations while maintaining computational efficiency and ease of implementation. Consequently, the method constitutes a reliable and efficient numerical framework that can be extended to a wide class of nonlinear partial differential equations arising in wave propagation phenomena.

Declarations

Acknowledgements: The author would like to express his sincere thanks to the editor and the anonymous reviewers for their helpful comments and suggestions

Author's Contribution: The author, D.S.Y., contributed to this manuscript fully in theoretic and structural points.

Conflict of Interest Disclosure: The author declares no conflict of interest.

Supporting/Supporting Organizations: This research received no external funding.

Ethical Approval and Participant Consent: This article does not contain any studies with human or animal subjects. It is declared that during the preparation process of this study, scientific and ethical principles were followed and all the studies benefited from are stated in the bibliography.

Plagiarism Statement: This article was scanned by the plagiarism program. No plagiarism detected.

Availability of Data and Materials: Data sharing not applicable.

Use of AI tools: The author declares that they have not used Artificial Intelligence (AI) tools in the creation of this article.

ORCID

Derya Yıldırım Sucu https://orcid.org/0000-0001-8396-8081

References

[1] J.V. Boussinesq, *Essai sur la theorie des eaux courantes (Essay on the theory of water flow)*, in: Memoires Presentes par Divers Savants à l'Academie des Sciences, **23** (1877), 241–680, Paris, France.

[2] D.J. Korteweg and G. de Vries, *On the change of form of long waves advancing in a rectangular canal, and on a new type of long stationary waves*, Philos. Mag., **39** (1895), 422–443. [Web]

[3] T.B. Benjamin, J.L. Bona and J.J. Mahony, *Model equations for long waves in nonlinear dispersive systems*, Philos. Trans. R. Soc. Lond. Ser. A, **272** (1972), 47–78. [CrossRef]

[4] D.H. Peregrine, *Calculations of the development of an undular bore*, J. Fluid Mech., **25**(2) (1966), 321–330. [CrossRef] [Scopus]

[5] D.H. Peregrine, *Long waves on a beach*, J. Fluid Mech., **27**(4) (1967), 815–827. [CrossRef] [Scopus]

[6] N.J. Zabusky, *A synergetic approach to problem of nonlinear dispersive wave propagation and interaction*, in: W. Ames (Ed.), Proc. Symp. Nonlinear Partial Differential Equations, Academic Press, 1967, 223–258. [CrossRef]

[7] B. Fornberg and G.B. Whitham, *A numerical and theoretical study of certain nonlinear wave phenomena*, Philos. Trans. R. Soc. Lond., **289** (1978), 373–404. [CrossRef] [Scopus]

[8] N.J. Zabusky and M.D. Kruskal, *Interaction of solitons in a collisionless plasma and the recurrence of initial states*, Phys. Rev. Lett., **15**(6) (1965), 240–243. [CrossRef] [Scopus]

[9] C.S. Gardner, J. M. Green, M. D. Kruskal and R. M. Miura, *Method for solving the Korteweg–de Vries equation*, Phys. Rev., **19** (1967), 1095. [CrossRef]

[10] T.B. Benjamin, J.L. Bona and J.J. Mahony, *Model equations for long waves in non-linear dispersive systems*, Phil. Trans. R. Soc. Lond. Ser. A, **272** (1972), 47–78. [CrossRef]

[11] L.R.T. Gardner, G.A. Gardner and A. Doğan, *A least squares finite element scheme for the RLW equation*, Commun. Numer. Methods Eng., **12**(11) (1996), 795–804. [CrossRef] [Scopus] [Web of Science]

[12] K. Omrani, *The convergence of the fully discrete Galerkin approximations for the Benjamin–Bona–Mahony (BBM) equation*, Appl. Math. Comput., **180** (2006), 614–621. [CrossRef] [Web of Science]

[13] K.R. Raslan, *A computational method for the regularized long wave (RLW) equation*, Appl. Math. Comput., **167**(2) (2005), 1101–1118. [CrossRef] [Web of Science]

[14] I. Dağ, B. Saka and D. Irk, *Galerkin method for the numerical solution of the RLW equation using quintic B-splines*, J. Comput. Appl. Math., **190**(1-2) (2006), 532–547. [CrossRef] [Scopus] [Web of Science]

[15] I. Dağ and M.N. Özer, *Approximation of the RLW equation by the least square cubic B-spline finite element method*, Appl. Math. Model., **25**(3) (2001), 221–231. [CrossRef] [Scopus] [Web of Science]

[16] A.A. Soliman and M.H. Hussien, *Collocation solution for RLW equation with septic spline*, Appl. Math. Comput., **161**(2) (2005), 623–636. [CrossRef] [Scopus] [Web of Science]

[17] P. Rosenau, *A quasi-continuous description of a nonlinear transmission line*, Phys. Scripta, **34**(6) (1986), 827–829. [CrossRef] [Scopus] [Web of Science]

[18] T. Ak, S.B.G. Karakoç and H. Triki, *Numerical simulation for treatment of dispersive shallow water waves with Rosenau–KdV equation*, Eur. Phys. J. Plus, **131**(10) (2016), 1–15. [CrossRef] [Scopus] [Web of Science]

[19] T. Ak, S. Dhawan, S.B.G. Karakoç, S.K. Bhowmik and K.R. Raslan, *Numerical study of Rosenau–KdV equation using finite element method based on collocation approach*, Math. Model. Anal., **22**(3)

(2017), 373–388. [CrossRef] [Scopus] [Web of Science]

[20] P. Rosenau, *Dynamics of dense discrete systems*, Prog. Theor. Phys., **79**(5) (1988), 1028–1042. [CrossRef] [Web of Science]

[21] M.A. Park, *On the Rosenau equation*, Math. Appl. Comput., **9** (1990), 145–152. [Web of Science]

[22] M.A. Park, *Pointwise decay estimate of solutions of the generalized Rosenau equation*, J. Korean Math. Soc., **29** (1992), 261–280.

[23] P.K. Barreta, C.S.Q. Caldas, P. Gamboa and J. Limaco, *Existence of solutions to the Rosenau and Benjamin–Bona–Mahony equation in domains with moving boundary*, Electron. J. Differ. Equ., **2004**(35) (2004), 1–12. [Scopus]

[24] S.K. Chung and S.N. Ha, *Finite element Galerkin solutions for the Rosenau equation*, Appl. Anal., **54**(2) (1994), 39–56. [CrossRef] [Scopus]

[25] S.K. Chung, *Finite difference approximate solutions for the Rosenau equation*, Appl. Anal., **69**(2) (1998), 149–156. [CrossRef] [Scopus]

[26] K. Omrani, F. Abidi, T. Achouri and N. Khiari, *A new conservative finite difference scheme for the Rosenau equation*, Appl. Math. Comput., **201**(2) (2008), 35–43. [CrossRef] [Scopus] [Web of Science]

[27] S.A.V. Manickam, A.K. Pani and S.K. Chung, *A second-order splitting combined with orthogonal cubic spline collocation method for the Rosenau equation*, Numer. Methods Partial Differ. Equ., **14**(6) (1998), 695–716. [CrossRef] [Scopus] [Web of Science]

[28] S.M. Choo, S.K. Chung and K.I. Kim, *A discontinuous Galerkin method for the Rosenau equation*, Appl. Numer. Math., **58**(6) (2008), 783–799. [CrossRef] [Scopus] [Web of Science]

[29] M.A. Helal, *Soliton solution of some nonlinear partial differential equations and its applications in fluid mechanics*, Chaos Solitons Fractals, **13**(9) (2002), 1917–1929. [CrossRef] [Scopus] [Web of Science]

[30] P. Rosenau and J.M. Hyman, *Compactons: Solitons with finite wavelength*, Phys. Rev. Lett., **70**(5) (1993), 564–567. [CrossRef] [Scopus] [Web of Science]

[31] F. Rus and F.R. Villatoro, *Self-similar radiation from numerical Rosenau–Hyman compactons*, J. Comput. Phys., **227**(1) (2007), 440–454. [CrossRef] [Scopus] [Web of Science]

[32] O.S. Iyiola, G.O. Ojo and O. Mmaduabuchi, *The fractional Rosenau–Hyman model and its approximate solution*, Alexandria Eng. J., **55**(2) (2016), 1655–1659. [CrossRef] [Scopus] [Web of Science]

[33] A. Ludu and J.P. Draayer, *Patterns on liquid surfaces: cnoidal waves, compactons and scaling*, Physica D, **123**(1-4) (1998), 82–91. [CrossRef] [Scopus] [Web of Science]

[34] A.S. Kovalev and M.V. Gvozdikova, *Bose gas with nontrivial particle interaction and semiclassical interpretation of exotic solitons*, Low Temp. Phys., **24**(7) (1998), 484–490. [CrossRef] [Scopus] [Web of Science]

[35] A.L. Bertozzi and M. Pugh, *The lubrication approximation for thin viscous films: regularity and long time behavior of weak solutions*, Commun. Pure Appl. Math., **49**(2) (1996), 85–123. [CrossRef] [Scopus] [Web of Science]

[36] V. Kardashov, S. Einav, Y. Okrent and T. Kardashov, *Nonlinear reaction–diffusion models of self-organization and deterministic chaos: theory and possible applications to description of electrical cardiac activity and cardiovascular circulation*, Discrete Dyn. Nat. Soc., **2006** (2006), 98959. [CrossRef] [Scopus] [Web of Science]

[37] J. de Frutos, M.A. Lopez-Marcos and J.M. Sanz-Serna, *A finite difference scheme for the K(2,2) compacton equation*, J. Comput. Phys., **120**(2) (1995), 248–252. [CrossRef] [Scopus] [Web of Science]

[38] F. Rus and F.R. Villatoro, *Pade numerical method for the Rosenau–Hyman compacton equation*, Math. Comput. Simul., **76**(1-3) (2007), 188–197. [CrossRef] [Scopus] [Web of Science]

[39] B. Mihaila, A. Cardenas, F. Cooper and A. Saxena, *Stability and dynamical properties of Rosenau–Hyman compactons using Pade approximants*, Phys. Rev. E, **81** (2010), 056708. [CrossRef]

[40] A. Cardenas, B. Mihaila, F. Cooper and A. Saxena, *Properties of compacton–anticompacton collisions*, Phys. Rev. E, **83**(6) (2011), 066705. [CrossRef] [Scopus] [Web of Science]

[41] P. Rosenau, *Compact and noncompact dispersive patterns*, Phys. Lett. A, **275**(3) (2000), 193–203. [CrossRef] [Scopus] [Web of Science]

[42] A. Chertock and D. Levy, *Particle methods for dispersive equations*, J. Comput. Phys., **171**(2) (2001), 708–730. [CrossRef] [Scopus] [Web of Science]

[43] D. Levy, C.W. Shu and J. Yan, *Local discontinuous Galerkin methods for nonlinear dispersive equations*, J. Comput. Phys., **196**(2) (2004), 751–772. [CrossRef] [Scopus] [Web of Science]

[44] M.S. Ismail and T.R. Taha, *A numerical study of compactons*, Math. Comput. Simul., **47**(6) (1998), 519–530. [CrossRef] [Scopus] [Web of Science]

[45] P. Saucez, A. Vande Wouwer, W.E. Schiesser and P. Zegeling, *Method of lines study of nonlinear dispersive waves*, J. Comput. Appl. Math., **168**(1-2) (2004), 413–423. [CrossRef] [Scopus] [Web of Science]

[46] R.Y. Molliq and M.S. Noorani, *Solving the fractional Rosenau–Hyman equation via variational iteration method and homotopy perturbation method*, Int. J. Differ. Equ., **2012** (2012), Article ID 472030. [CrossRef] [Scopus] [Web of Science]

[47] A. Akgül, A.I. Aliyu, M. Inç, A. Yusuf and D. Baleanu, *Approximate solutions to the conformable Rosenau–Hyman equation using the two-step Adomian decomposition method with Padé approximation*, Math. Methods Appl. Sci., **43**(13) (2020), 7632–7639. [CrossRef] [Scopus] [Web of Science]

[48] S.O. Ajibola, A.S. Oke and W.N. Mutuku, *LHAM approach to fractional order Rosenau–Hyman and Burgers' equations*, Asian Res. J. Math., **16**(6) (2020), 1–4. [Web]

[49] F. Mirzaee and N. Samadyar, *Combination of finite difference method and meshless method based on radial basis functions to solve fractional stochastic advection–diffusion equations*, Eng. Comput., **36**(4) (2019), 1673–1686. [CrossRef] [Scopus] [Web of Science]

[50] N. Samadyar, Y. Ordokhani and F. Mirzaee, *The couple of Hermite-based approach and Crank–Nicolson scheme to approximate the solution of the two-dimensional stochastic diffusion–wave equation of fractional order*, Eng. Anal. Bound. Elem., **118** (2020), 285–294. [CrossRef] [Scopus] [Web of Science]

[51] F. Mirzaee and N. Samadyar, *Parameters estimation of HIV infection model of $CD4^+$ T-cells by applying orthonormal Bernstein collocation method*, Int. J. Biomath., **11**(02) (2018), 1850020. [CrossRef] [Scopus] [Web of Science]

[52] H. Dehestani, Y. Ordokhani and M. Razzaghi, *On the applicability of Genocchi wavelet method for different kinds of fractional-order differential equations with delay*, Numer. Linear Algebra Appl., **26**(5) (2019), e2259. [CrossRef] [Scopus] [Web of Science]

[53] H. Dehestani, Y. Ordokhani and M. Razzaghi, *Combination of Lucas wavelets with Legendre–Gauss quadrature for fractional Fredholm–Volterra integrodifferential equations*, J. Comput. Appl. Math., **382** (2021), 113070. [CrossRef] [Scopus]

[54] S. Kumbinarasaiah, *Numerical solution for the $(2+1)$-dimensional Sobolev and regularized long wave equations arising in fluid mechanics via wavelet technique*, Partial Differ. Equ. Appl. Math., **3** (2021), 100016. [CrossRef] [Scopus]

[55] S. Kutluay, N.M. Yağmurlu and A.S. Karakaş, *A new perspective for simulations of equal-width wave equation*, Comput. Methods Differ. Equ., (2025). [CrossRef]

[56] S. Kutluay, N.M. Yağmurlu and A.S. Karakaş, *A novel perspective for simulations of the modified equal-width wave equation by cubic Hermite B-spline collocation method*, Wave Motion, **129** (2024), 103342. [CrossRef] [Scopus] [Web of Science]

[57] P.M. Prenter, *Splines and Variational Methods*, John Wiley & Sons, New York, U.S.A., (1975). [Web]

[58] S.K. Bhowmik, R. Belbakir, T.Z. Boulmezaoud and S. Mziou, *Solving two-dimensional second-order elliptic equations in exterior domains using the inverted finite elements method*, Comput. Math. Appl.,

67(10) (2014), 2027–2038.

[59] S.K. Bhowmik and A.K. Jakobin, *High-accurate numerical schemes for Black–Scholes models with sensitivity analysis*, J. Math., **2022** (2022), Article ID 4488082. [CrossRef] [Scopus] [Web of Science]

[60] H. Gomez and L. De Lorenzis, *The variational collocation method*, Comput. Methods Appl. Mech. Engrg., **309** (2016), 152–181. [CrossRef] [Scopus] [Web of Science]

[61] S.K. Bhowmik, *Piecewise polynomial approximation of a nonlocal phase transitions model*, J. Math. Anal. Appl., **420**(2) (2014), 1069–1094. [CrossRef] [Scopus] [Web of Science]

[62] S. Dhawan, S.K. Bhowmik and S. Kumar, *Galerkin least-square B-spline approach toward advection–diffusion equation*, Appl. Math. Comput., **261** (2015), 128–140. [CrossRef] [Scopus] [Web of Science]

[63] T. Ak, S. Dhawan, S.B.G. Karakoç, S.K. Bhowmik and K.R. Raslan, *Numerical study of Rosenau–KdV equation using finite element method based on collocation approach*, Math. Modelling Anal., **22**(3) (2017), 373–388. [CrossRef] [Scopus] [Web of Science]

[64] M. Çınar, A. Seçer and M. Bayram, *An application of Genocchi wavelets for solving the fractional Rosenau–Hyman equation*, Alexandria Eng. J., **60**(6) (2021), 5331–5340. [CrossRef] [Scopus] [Web of Science]

[65] S. Kumbinarasaiah and M. Mulimani, *The Fibonacci wavelets approach for the fractional Rosenau–Hyman equations*, Results Control Optim., **11** (2023), 100221. [CrossRef] [Scopus] [Web of Science]

Advances in Analysis and Applied Mathematics (AAAM), (Adv. Anal. Appl. Math.)
https://advmath.org/index.php/pub

How to cite this article: D. Yıldırım Sucu, *High-accuracy finite element modeling of the Rosenau–Hyman equation*, Adv. Anal. Appl. Math., **2**(2) (2025), 119-131. DOI 10.62298/advmath.36